



Design of peer-to-peer energy trading in transactive energy management for charge estimation of lithium-ion battery on hybrid electric vehicles

Subramanian Annamalai^a, S.P. Mangaiyarkarasi^{b,*}, M.Santhosh Rani^c, V. Ashokkumar^d,
Deepak Gupta^{e,f}, Joel JPC. Rodrigues^{f,g}

^a Department of Electrical and Electronics, Srinivasa Ramanujan Centre, Sastra Deemed to be University, Kumbakonam, 612001, India

^b Department of Electrical and Electronics Engineering, University College of Engineering, Panruti, Tamilnadu, 607106, India

^c Department of Mechatronics Engineering, SRM Institute of Science and Technology, Kattankulathur, Tamil Nadu 603203, India

^d Department of Electrical and Electronics Engineering, K.Ramakrishnan College of Engineering, Tiruchirappalli-621112, India

^e Maharaja Agarsen Institute of Technology, New Delhi, India

^f Federal University of Piauí (UFPI), Teresina, PI, Brazil

^g Instituto de Telecomunicações, Covilhã, Portugal

ARTICLE INFO

Keywords:

Transactive energy management
Peer-to-peer energy trading
Battery management
Energy efficiency
SOC estimation
Machine learning

ABSTRACT

Transactive energy is a next big thing in the energy sector which considerably transform the association between utility, consumer, and the environment. Transactive energy management (TEM) system comprises a collection of economical and controlling strategies which helps to dynamically balance the power infrastructure. Peer-to-Peer (P2P) trading becomes familiar, which mainly based on the process of power generation and consumption is completely decentralized. At the same time, Hybrid electric vehicles (HEV) have become an important technology to accomplish energy efficiency and environmental sustainability. Battery Management System (BMS) evaluates the power and State of Charge (SOC), confirms the well-being depending upon the measurement. Accurate SOC estimation is crucial to ensure the unflinching functioning of Li-ion battery that is mainly employed in HEVs. A reliable SOC prediction model is needed to assure the precise measurement of the residual driving range of the vehicle and appropriate battery balancing. In this view, this paper presents an optimal machine learning based SOC estimation (OML-SOCE) model for HEVs in TEM. The OML-SOCE is aimed for estimating an accurate capacity of SOC of Li-ion batteries on HEVs. The OML-SOCE technique involves a two stage process namely stacked sparse autoencoder (SSAE) based prediction and salp swarm algorithm (SSA). At the first stage, SSAE is used for the prediction of SOC. Sparse auto-encoder (AE) is an enhanced AE technique that improves any some sparsity restrictions in the hidden layer of standard AE. A stack of multiple sparse AE forms a deep network framework that is named as SSAE. Next, in the second stage, the parameters involved in the SSAE are optimally adjusted by the use of SSA in such a way that the prediction performance can be considerably improved. A wide range of experiments take place and the results are investigated under varying temperature levels. The experimental outcomes showcased the supremacy of the presented technique the recent techniques with respect to different measures.

1. Introduction

Transactive energy market (TEM) remains an important research area, which is commonly applied to balance the dynamic supply and demand over the grids. It enables the Peer-to-Peer (P2P) energy trading which creates a connection between the consumer as well as prosumer to trade energy with one another. The P2P energy improves the flexibility by reducing the user demand and minimizing the burden on the

network. On the other hand, Lithium-Ion batteries are commonly employed in Hybrid Electric Vehicle (HEV) and Electric Vehicle (EV) because of their numerous benefits on other kinds of batteries [1]. It has the special characteristic that needs a Battery Management System (BMS) for dynamically monitoring its parameter, in addition, to guarantee the safe, reliable, and control operations of battery at the time of their discharging or charging cycle [2, 3]. The primary objective of the BMS is to control and monitor the battery processes like discharging

* Corresponding author.

E-mail address: mangai@ucep.edu.in (S.P. Mangaiyarkarasi).

<https://doi.org/10.1016/j.epsr.2022.107845>

Received 6 October 2021; Received in revised form 31 January 2022; Accepted 1 February 2022

Available online 10 February 2022

0378-7796/© 2022 Elsevier B.V. All rights reserved.

cycle and charging cycle, assure the health conditions of the battery, minimizing the possibility of battery damage by assuring optimized energy is being delivered from the battery to power the vehicle [4]. The monitoring circuits in BMS are employed for monitoring the key characteristics of the battery such as current, voltage, temperature at discharging, and charging conditions for ensuring the safe operation [5].

State of Charge (SOC) is a significant parameter determining the state of a Li-ion battery. SOCs are determined as the ratio of battery's residual to the nominal capacity. As the over-discharging and -charging brings unavoidable harm to a Li-ion battery, precise SOC prediction must be given as the BMS. The more commonly applied approach for SOC predictions is Coulomb counting [6]. Nonetheless, prediction error might be gathered for open-loop approach, results in the prediction drifting far from the accurate value. Also, Early SOC errors cause biases in the prediction. Another widely utilized methods are the open-circuit-voltage (OCV) technique. This technique attains SOC from the battery's OCV-SOC relationships [7]. But, precise OCV measurements require the batteries should be in state of equilibrium when the battery in EV is at operation in the course of driving. Hence, the OCV approach isn't applicable for realtime SOC prediction.

Approaches including classical Machine Learning (ML) method were employed in the previous. The benefit of this type of method is that they could be trained using realworld data and self-learn SOC prediction without needing handcrafted model [8]. But, if NNs are exclusively utilized, the outcomes are typically not sufficiently precise, and hence needed the further usage of Kalman filter or another inference approaches for achieving adequate prediction accuracy. Even though few studies have employed Kalman filter in conjunction with equivalent circuit battery models/integrated battery models, also various studies have employed in conjunction using NN battery model. In [9], a trained two layer NN with thirty neurons in the hidden layer estimate terminal voltage about 4% RMS errors [10]. Moreover, the ELM approach is trained on constant discharge pulse therefore the efficiency in transient load demand, experienced in realtime situations, isn't known. In subtractive clustering and FC means methods are employed using an SVM for SOC prediction. The study was executed is based on the last fuzzy SVM method with a GA based FC means clustering approach using a BP technique for estimating SOC and is stated to surpass traditional fuzzy modeling approaches.

1.1. Motivation

In recent years, the P2P energy trading improves the flexibility by reducing the user demand and minimizing the burden on the network. Previous studies have used statistical and machine learning models for battery SOC prediction in TEM. These approaches use a moving average prediction with a decreased electrochemical method that is capable of performing prediction without linearization error and permits for constraint on states such as Li-ion concentration and internal resistance state [11]. Though several approaches are existed in the literature, there is still needed to design OML-SOCE technique for SOC estimation of Li-ion batteries in TEM.

1.2. Objectives

The major objective of this study is to design an automated machine learning based prediction model for SOC estimation of Li-ion batteries on HEVs in TEM.

1.3. Paper contribution

This paper presents an optimal machine learning based SOC estimation (OML-SOCE) model for HEVs for estimating an accurate capacity of SOC of Li-ion batteries on HEVs in TEM. The OML-SOCE technique involves a two-stage process namely stacked sparse autoencoder (SSAE) based prediction and salp swarm algorithm (SSA). Sparse auto-encoder

(AE) is an enhanced AE technique that improved any sparsity restrictions in the hidden layer of traditional AE. Besides, the parameters involved in the SSAE are optimally adjusted by the use of SSA in such a way that the prediction performance can be considerably improved. A comprehensive simulation analysis is carried out and the outcomes are inspected under distinct temperature levels.

1.4. Paper organization

The rest of the paper is organized as follows. Section 2 offers a detailed literature review and Section 3 introduces the proposed OML-SOCE technique. In addition, Section 4 offers the detailed experimental validation and Section 5 draws the conclusion of the study.

2. Related works

Chandran et al. [12] introduce the SoC predicting of Li-ion battery system through 6 ML methods for EV applications. The applied algorithm consists of ANN, SVM, LR, GPR, EBA, and EBo. Error analyses of the models are performed for optimizing the battery's efficiency. In Hannan et al. [13], the capability of optimized ML technique is proposed for enhancing SOC prediction based on accuracy, learning capability, convergence speed, and generalization performance. Also, authenticate the presented algorithm using noise, Li-ion batteries experiment, EV drive cycle, aging effect, and temperature. Sidhu et al. [14] introduce an enhanced SOC prediction of Li-ion battery using RF approach, i.e., effective and robust to control dynamic system. For ensuring better accuracy and good resilience, Gaussian filters are adapted at the concluding phase for minimizing the variation in the SOC prediction. The presented SOC estimators are tested on the investigational data of the Li-ion battery in distinct operating temperatures and Federal test driving schedules.

Zhang et al. [15] proposed a compact RBF neural method for predicting SOC approach of lithium battery packs. Initially, an appropriate input set powerfully related to the package SOC is recognized from directly measured current, temperature, and voltage signals using an FRA strategy. Next, an RBF neural method for battery pack SOC estimations is made by the FRA approach for pruning unwanted hidden layer neurons. Later, the PSO approach is employed for optimizing the kernel parameter. Lastly, a traditional RBF NN method, an enhanced RBF neural method with the 2 phase methods, and also LSSVM models are employed for estimating the battery SOC as a comparative analysis.

In Xu et al. [16], a new method integrating Sigma-point Kalman filters and ML method depending on equivalent circuit models are presented for improving the SOC prediction accuracy of a reutilized battery pack (LiFePO₄) by reducing the negative effects of hysteresis phenomenon. In Tian et al. [17], DNN based methods are presented for estimating SOC by current data and 10-min charging voltage as the input. Therefore, it could be employed for calibrating the SOC prediction for the Ampere hour counting technique. Also, demonstrates that by integrating the DNN method to Kalman filters, the strength of SOC prediction against error spikes and arbitrary noise could be enhanced.

Anjum et al. [18] have recognized a minimum configuration of a DNN framework and hyper parameters setting to efficiently predict SOC of EV battery cells. The experimental result shows that a minimum configuration of hidden neurons and layers could decrease the resource and computation costs needed without compromising efficiency. Additionally, it is assisted by several epochs for training optimal DNN SOC estimation models. In Zahid et al. [19], a SOC prediction method with subtractive clustering based neuro fuzzy systems are evaluated and presented using the experiment with an innovative vehicle simulator compared to BPNN and ENN methods.

Chemali et al. [20] introduce a novel technique for performing precise SOC estimations for Li-ion batteries via an RNN using LSTM. Showcases the LSTM-RNN capability for encoding dependency in time and precisely predict SOC without the use of inference systems, battery

models, filters such as Kalman filters. Additionally, ML techniques, such as each other, can able to generalize the abstraction it learns at the time of training for another dataset taken in distinct situations. Hence, they exploit this feature by training an LSTM-RNN method on dataset noted at several ambient temperatures. In Wei et al. [21], the approach of the dynamic NN is applied for predicting the SOC of Li-ion battery, i.e., enhanced according to the classical close-loop non-linear autoregressive model using NARXNN method, and the open-loop NARXNN models consider anticipated outputs are presented. As the feedback delay, input delay, and hidden layers of the dynamic NN are generally elected empirically, that affect the prediction efficiency of the dynamic NN.

3. The proposed OML-SOCE technique

In this study, a new OML-SOCE technique is derived for the SOC estimation of the Li-ion battery in HEVs. The OML-SOCE technique includes SSAE based predictive model to determine the proper level of SOC. Besides, the parameter optimization of the SSAE model takes place using the SSA.

3.1. Problem formulation

Consider a group of positions $l \in L, L = L_P \cup L_{P^-}$ which could be charging station (viz., L_P) or not (viz., L_{P^-}). Depending upon this, they determine a transportation network as a graph $G=(E, L)$ together node L & edge E , whereas $e \in E$ denotes road and $l \in L$ indicates junction of road network. They determine distinct time points $t \in T, T \subseteq \mathbb{N}$ when they represent the group of EVs as $a \in A$.

Here, $\forall l \in L_P$ has several charging slots $s_l \in \mathbb{N}$. All the charging stations l have a charging rate, $c_l \in \mathbb{R}_0^+$ and each charging station has a set cost $cost_l^{elec} \in \mathbb{N}$ for paying the electricity supplier to all the units of electricity. Therefore, they determined a matrix allocation charge $_{a,l,t} \in \{0,1\}$ for representing EV a is at charging station l in time point t . Furthermore, all the charging stations have an estimated demand $dem_{l,t} \in \mathbb{N}$ for every time point that is considered to be fixed with the electrical energy supplier beforehand. A monetary penalty $cost_{l,t}^{imbl}$

$$cost_{l,t}^{imbl} = \left| \sum_a charge_{a,l,t} - dem_{l,t} \right| \times cost^{imbl} \quad (1)$$

is employed for the station when the actual demand differs from the predictable one [24]. The variance in the complete values are the imbalance regarding utilized energy and $cost^{imbl}$ is a set price the station pays to the electrical energy supplier if the actual demand is distinct from the predicted one. Hence, index a denotes EVs, l to the charging station, and t indicates time point.

Every EVs a is assumed as an autonomous agent and has a kind $\theta_a = \langle d_a, b_a^{(max)}, b_a(t), l_a^{start}, t_a^{start}, l_a^{end}, \tau_a^{prk}, t_a^{arr}, t_a^{l}^{dep}, b_a^{chrg}, v_a^{elec} \rangle$. All a have a discharge rate $d_a \in \mathbb{R}_0^+$, a maximal battery capability $b_a^{(max)} \in \mathbb{R}_0^+$, also a present battery levels in time $t, b_a(t) \in \mathbb{R}_0^+$ estimated in kWh. Furthermore, all EV a start out from their source position l_a^{start} at time $t_a^{start} \in T$ and should travel to terminus l_a^{end} where it should park at time $\tau_a^{prk} \in \mathbb{N}$. Assume pairs of locations (l_a^{start}, l_a^{end}) and transport network G , shortest route, $r_l(l_a^{start}, l_a^{end}) \in \mathbb{R}(l_a^{start}, l_a^{end})$ from the source to destination is estimated by Dijkstra method. Likewise, the shortest route $r_l(l_a^{start}, l_a^{end}) \in \mathbb{R}(l_a^{start}, l_a^{end})$ from the sources to the whole charging points $l \in L_P$ are estimated. All the routes $r_l(l_a^{start}, l_a^{end})$ have a distance $\delta_l(l_a^{start}, l_a^{end})$ calculated in kilometers, a time to travel $\tau_l(l_a^{start}, l_a^{end})$ drive: $\mathbb{R}(l_a^{start}, l_a^{end}) \rightarrow \mathbb{N}$ and a quantity of energy desired, $\epsilon_l(l_a^{start}, l_a^{end})$ need $(\tau_l(l_a^{start}, l_a^{end}) \text{ drive}, d_a)$. Depending upon slot availability and capability of EV for attaining a charging point with its early battery level, a group of usable charging point $\Gamma_a(a, t) \subseteq L_P$ is determined. All the EVs are presented for charging among $t_a^{l}^{arr} = t_a^{start} + \lceil \tau_l(l_a^{start}, l_a^{end}) \text{ drive} \rceil$ and $\lceil t_a^{l}^{dep} = t_a^{l}^{arr} + \tau_l(l_a^{start}, l_a^{end}) \text{ prk} \rceil$. Noted that τ_l drive is estimated depending

upon the distance to location l separated with an average speed. All the vehicles should charge a certain quantity of energies $b_a^{chrg} \leq b_a^{(max)}$ in charging point l and have private valuations $v_a(l)$ to charge the desirable quantity of energies in all the charging points.

All the EVs have a private valuation to charge the desirable quantity of electricity in a certain position.

$$v_{a,l} = \begin{cases} (v_a^{elec} - \kappa_{a,l}^{time}) \times b_a^{chrg}, & \text{if } b_{a,t} \text{ dep}_{a,l} \geq b_a^{chrg} \\ 0, & \text{otherwise} \end{cases} \quad (2)$$

Based on Eq. (2), a time cost $\lceil \kappa_{a,l} \rceil$ time linked to drive for the station and walk from the station to the ending is subtracted in valuation v_a^{elec} to charge one unit of electricity. v_a^{elec} and $\kappa_{a,l}$ are with zero and one range. Noted that $\kappa_{a,l}$ is processed equally for the whole agents since it is depending upon graph which is utilized for representing the road network. Noted that the agent has 0 valuations to charge lesser compared to b_a^{chrg} , and valuation $v_a(l)$ to charge equivalent to above b_a^{chrg} . Furthermore, all the agent a obtains utility u_a ,

$$u_a = v_{a,l} - p_a \quad (3)$$

Whereas $p_a \in \mathbb{R}$ denotes monetary transmit from EV to systems (viz., the utility is an amount of fulfillment to charge the desirable quantity of electricity). p_a is generally positive, since the EV pays the charging station for electricity. But, the event of charging EV results in low imbalance cost to charging station, the transmission for this EV might be negative. It should disclose its kind θ_a to the scheme. Later, the scheme employs an EV to charge station distribution method for scheduling EV charging and utilizes each projected pricing mechanism for calculating the price.

3.2. SSAE based predictive model

The proposed method aims to model an efficient SOC evaluation approach for battery management in HEV. Initially, the output and input variables included in the proposed method are defined. Based on the HEV, the SOC undergoes sampling at step k , $SOC(k)$, which is determined by the module input as it denotes the batteries existing condition. The SOC is a non-linear connection with the dominant factors, such as current and battery voltage. The proposed model can able to describe these connections accurately. Therefore, the straightaway measure parameter, current $I(k)$ represents the input and the output $V(k)$ signifies the battery terminal voltage. Furthermore, the terminal voltage at the sample steps $-1, V(k-1)$, are further elected as the 3rd input to presented approach. $V(k-1)$ means the battery's condition at last step and signifies the beforehand working condition. The concepts exist in the choice of $V(k-1)$ is the process of respective circuit method to Li-ion battery [21]. The terminal voltage at k steps are determined by Eq. (4):

$$V(k) = OCV(SOC(k)) + R_s I(k) + U_{RC}(k) \quad (4)$$

whereas R_s refers the battery internal resistance, $U_{RC}(k)$ implies the RC circuit voltage connect to $U_{RC}(k-1)$ with the 1-order differential equation. For making the approach input straightaway defined parameter, $U_{RC}(k-1)$ is considered as included in $V(k-1)$. Hence, $V(k-1)$ has direct connection with $V(k)$. The function is obtained by the syncretization of the hidden parameters

$$V(k) = f(V(k-1), I(k), SOC(k)), \quad (5)$$

which undergoes estimation using learning systems. The input and output vectors for the presented battery method is characterized as $p(k) = [V(k-1) \ I(k) \ SOC(k)]^T$ & $V(k)$. It is arithmetically determined by:

$$F(p(k)) = V(k) \quad (6)$$

The input-output samples of $\{p(k) \sim V(k)\}$ are achieved by the

simulation previous to model training. Define $p(k)=x_j$ & $V(k)=t_j$. The training sets could be denoted as $\{(x_j, t_j) | x_j \in R^n, t_j \in R^m, j=1, \dots, N\}$. At these conditions, $n=3$, $m=1$, N indicates the amount of instance which present in the training data. Therefore, SSAE is used for prediction purposes.

The SSAE has been NN included of several SAEs linked from the end-to-end way. The outcomes of the previous layer of sparse self-encoding have been employed as the input of succeeding layer of self-encoding, so high level features illustration of input data were obtained. The greedy layerwise pre-trained technique has been employed to sequential trained of every layer of SSAE to retrieve the optimize association weights as well as bias values of the entire SSAE networks. Afterward, the error BP approach has been developed to fine-tuned the SSAE till the resultant of error function amongst the input as well as output data fulfills the expected necessities, for getting an optimum parameter technique. The error function $J_{sparse}(W, b)$ is determined by:

$$\frac{\partial}{\partial w_{ij}^r} J_{sparse}(W, b) = \frac{1}{2n_r} \sum_{r=1}^{n_r} \frac{\partial}{\partial w_{ij}^r} J_{sparse}(W, b, X(n), Y(n)) + \lambda w_{ij}^r \quad (7)$$

$$\frac{\partial}{\partial b^r} J_{sparse}(W, b) = \frac{1}{2n_r} \sum_{r=1}^{n_r} \frac{\partial}{\partial b^r} J_{sparse}(W, b, X(n), Y(n)) \quad (8)$$

Therefore, the upgraded manner of the weight and bias are provided as:

$$w_{ij}^k = w_{ij}^k - \eta \frac{\partial}{\partial w_{ij}^k} J(W, b) \quad (9)$$

$$b^r = b^r - \eta \frac{\partial}{\partial b^r} J(W, b) \quad (10)$$

Where $X(n)$ and $Y(n)$ are correspondingly represents as n th actual vector and corresponding reformation vectors, and η stands for the upgraded

learning rate [22].

Let sparse restraint in the SSAE technique, it essential employing many rates of learning to distinct parameters as reducing the frequency of upgrading for infrequent feature. Fig. 1 depicts the framework of SSAE [21]. However, the standard Gradient Descent (GD) approach has of Stochastic Gradient Descent (SGD) as well as mini-batch GD which employ an identical rate of learning for all the network parameters that need for upgrading, generating it difficult for choosing the proper rate of learning and simply gain the local minimal.

3.3. SSA based parameter optimization

For boosting the SOC estimation performance of the SSAE technique, the SSA is used to optimally modify the parameters involved in the SSAE model. SSA has been current bio-inspired optimized algorithm [23], simulated as navigation and foraging performance of salp chain, usually initiate in Deep Ocean. From the mathematical process, salp population has been separated as to 2 groups named leaders and followers. An optimum salp (optimum solution) has assumed that food source that subsequently the salp chain. Then all iterations, the leader salp modifies their place in terms of the feed source. The leader explore as well as exploit the search space about the optimum solution and follower salps move slowly nearby leaders. This procedure assists salp from converging to global optimum rapidly but avoiding it from being trapped from local optimum.

The salp places were determined in the n -dimension search space: Where n implies the amount of decision variable from this issue.

Considered that the food source $\mathbb{F}S$ under the search space as swarm targets. As per the place of food source, leader upgrades their place utilizing the Eq. (11):

$$x_j^1 = \begin{cases} \mathbb{F}S_j + C_1 \times [\mathbb{U}b_j - \mathbb{L}b_j C_2 + \mathbb{L}b_j], & C_3 \geq 0 \\ \mathbb{F}S_j - C_1 \times [\mathbb{U}b_j - \mathbb{L}b_j C_2 + \mathbb{L}b_j], & C_3 < 0 \end{cases} \quad (11)$$

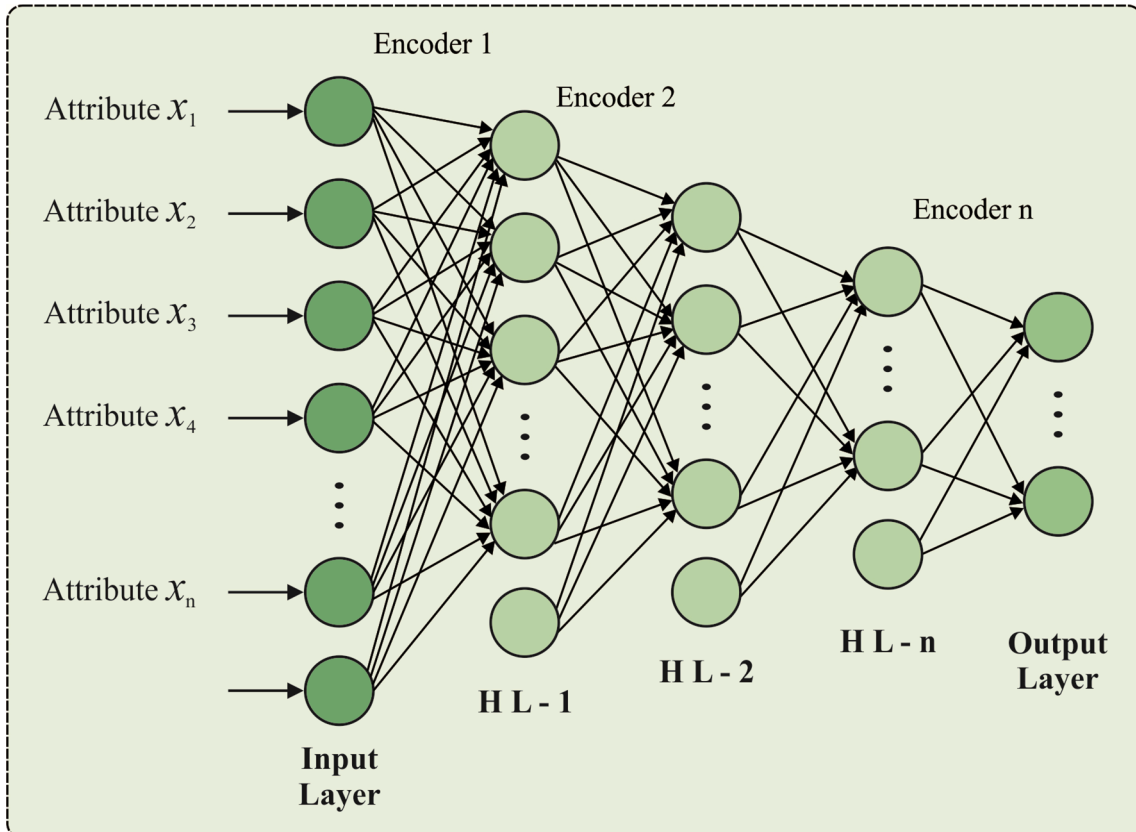


Fig. 1. Structure of SSAE.

The balance amongst exploration as well as exploitation in optimization is continued by coefficient C₁ determined as:

$$C_1 = 2 \times e^{-\left[\frac{4 \times \text{iter} - c}{\text{iter} - \text{max}}\right]^2} \quad (12)$$

At this point, iter_c represents the present iteration number and iter_{max} refers the maximal amount of iterations permitted, C₂ and C₃ are the uniformly distributed arbitrary numbers from the interval 0 and 1. Fig. 2 showcases the flowchart of SSA.

In SSA, followers upgrade their places as per Newton’s law of motion:

$$x_j^i = \frac{1}{2} \alpha t^2 + w_0 t, \quad i \geq 2 \quad (13)$$

Where;

$$\alpha = \frac{w_{final}}{w_0} \quad (14)$$

and

$$w = \frac{x - x_0}{t} \quad (15)$$

Assuming, w₀=0 and as the variance amongst some 2 consecutive time steps is 1, so

$$x_j^i = \frac{1}{2} \times (x_j^i + x_j^{i-1}); \quad i \geq 2 \quad (16)$$

The parameter optimization problem of SSAE can be optimally solved by the SSA and consequently, the prediction outcome is enhanced.

4. Performance validation

During this analysis, Dynamic Stress Test (DST) and Federal Urban Driving Schedule (FUDS) effort profiles have been utilized to test the projected method at 3 distinct temperatures. These effort cycles holds a diversity of present current profiles interms of distinct amplitude and time intervals with regenerative charging. The time period contained to complete 1-cycle of DST and FUDS is 360 s and 1372s correspondingly. For validating the projected approach, the data is gathered in CALCE

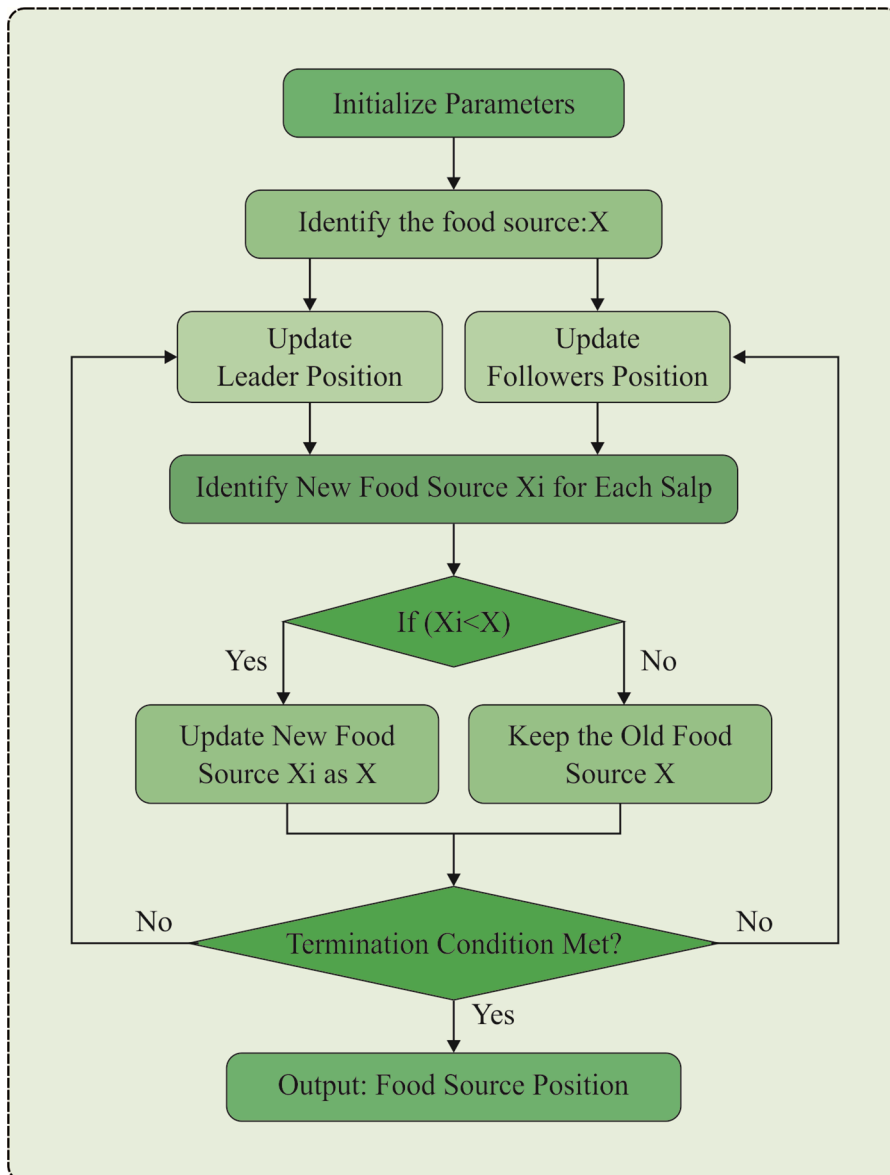


Fig. 2. Flowchart of SSA.

battery group. The CALCE gained the data in customized made battery test bench. The readings are taken at diverse temperatures at 0 °C, 25 °C, and 45 °C respective. The group of 3 important factors contained are voltage, current, and temperature. The election of 3 features are logical as current, voltage, and temperature are considerable control on battery outcomes.

Fig. 3 investigates the RMSE analysis of the OML-SOCE technique for SOC estimation process at varying temperature. The figure depicted that the OML-SOCE technique has accomplished effective outcome with the minimal RMSE value under all temperature values. On the applied DST cycle, the OML-SOCE technique has resulted to a lower RMSE of 1.24, 0.73, and 0.38 under 0 °C, 25 °C, and 45 °C correspondingly. Similarly, under FUDS cycle, the OML-SOCE technique has accomplished to a reduced RMSE of 1.53, 0.82, and 0.31 under 0 °C, 25 °C, and 45 °C correspondingly.

Fig. 4 examines the MAE analysis of the OML-SOCE approach for SOC estimation process at varying temperature. The figure exhibited that the OML-SOCE manner has accomplished effectual result with the minimum MAE value under all temperature values. On the applied DST cycle, the OML-SOCE manner has resulted to a lesser MAE of 0.68, 0.43, and 0.28 under 0 °C, 25 °C, and 45 °C correspondingly. Also, under FUDS cycle, the OML-SOCE methodology has accomplished to a minimal MAE of 0.81, 0.45, and 0.32 under 0 °C, 25 °C, and 45 °C correspondingly.

Fig. 5 explores the MAPE analysis of the OML-SOCE manner for SOC estimation process at distinct temperature. The figure exhibited that the OML-SOCE approach has accomplished effectual outcome with the lesser MAPE value under all temperature values. On the applied DST cycle, the OML-SOCE approach has resulted to a minimal MAPE of 9.52, 6.56, and 4.10 under 0 °C, 25 °C, and 45 °C correspondingly. Eventually, under FUDS cycle, the OML-SOCE approach has accomplished to a decreased MAPE of 18.53, 11.87, and 9.21 under 0 °C, 25 °C, and 45 °C correspondingly.

A brief RMSE results analysis of the OML-SOCE technique for SOC estimation in DST cycle is displayed in Fig. 6. The figure reported that the OML-SOCE technique has resulted to an effective outcome with the least RMSE. On the applied 0 °C, the OML-SOCE technique has accomplished to a lower RMSE of 1.24 but the RBFNN- BSA, GRNN-BSA, ELM-BSA, and BPNN- BSA techniques have obtained a higher RMSE of 1.95, 2.37, 2.46, and 1.47 respectively. Besides, on the applied 25 °C, the OML-SOCE manner has accomplished to a minimal RMSE of 0.73 but the RBFNN- BSA, GRNN-BSA, ELM- BSA, and BPNN- BSA algorithms have reached a superior RMSE of 1.23, 2.13, 1.86, and 0.81 correspondingly. Moreover, on the applied 45 °C, the OML-SOCE method has accomplished to a least RMSE of 0.38 but the RBFNN- BSA, GRNN-BSA, ELM-

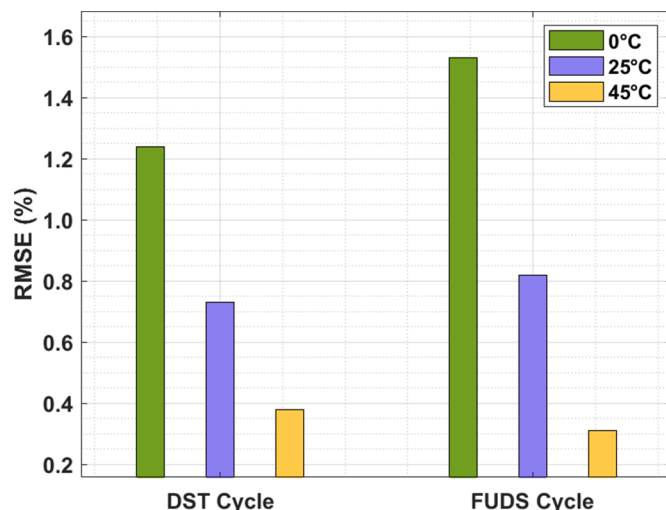


Fig. 3. Result analysis of OML-SOCE model interms of RMSE.

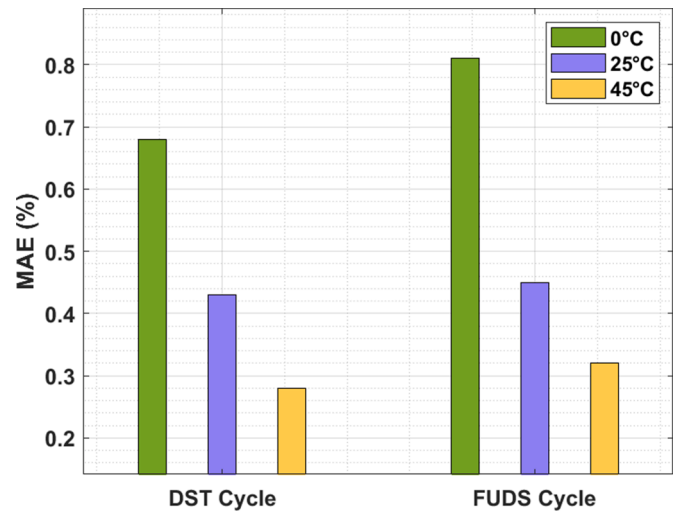


Fig. 4. Result analysis of OML-SOCE model interms of MAE.

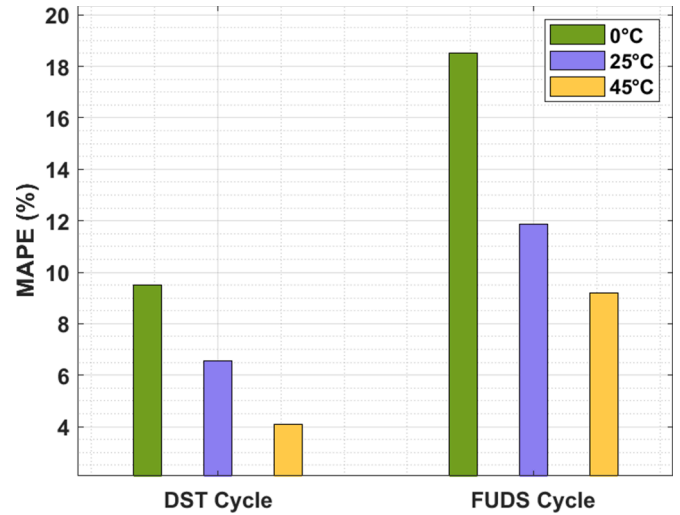


Fig. 5. Result analysis of OML-SOCE model interms of MAPE.

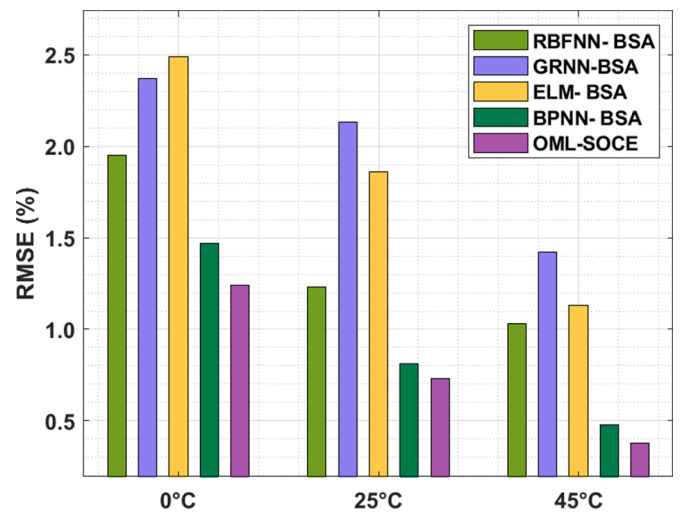


Fig. 6. RMSE analysis of OML-SOCE model under DST cycle.

BSA, and BPNN- BSA methodologies have reached a superior RMSE of 1.03, 1.42, 1.13, and 0.48 correspondingly.

A detailed MAPE outcomes analysis of the OML-SOCE manner for SOC estimation in DST cycle is showcased in Fig. 7. The figure stated that the OML-SOCE manner has resulted to an effectual outcome with the least MAPE. On the applied 0 °C, the OML-SOCE technique has accomplished to a lesser MAPE of 9.52 but the RBFNN- BSA, GRNN-BSA, ELM- BSA, and BPNN- BSA algorithms have achieved an increased MAPE of 21.62, 30.24, 24.93, and 9.84 correspondingly. Moreover, on the applied 25 °C, the OML-SOCE method has accomplished to a lower MAPE of 6.56 but the RBFNN- BSA, GRNN-BSA, ELM- BSA, and BPNN- BSA techniques have obtained a higher MAPE of 14.58, 23.39, 18.47, and 5.07 respectively. Additionally, on the applied 45 °C, the OML-SOCE approach has accomplished to a minimum MAPE of 4.10 but the RBFNN- BSA, GRNN-BSA, ELM- BSA, and BPNN- BSA algorithms have gained a maximum MAPE of 8.98, 14.36, 12.29, and 5.07 correspondingly.

A briefly RMSE results analysis of the OML-SOCE method for SOC estimation in FUDS cycle is depicted in Fig. 8. The figure demonstrated that the OML-SOCE technique has resulted to an effective outcome with the least RMSE. On the applied 0 °C, the OML-SOCE technique has accomplished to a minimal RMSE of 1.53 but the RBFNN- BSA, GRNN- BSA, ELM- BSA, and BPNN- BSA manners have achieved an improved RMSE of 3.58, 3.22, 3.72, and 1.74 respectively. Followed by, on the applied 25 °C, the OML-SOCE technique has accomplished to a method RMSE of 0.82 but the RBFNN- BSA, GRNN-BSA, ELM- BSA, and BPNN- BSA approaches have attained an increased RMSE of 2.23, 2.17, 2.34, and 0.91 respectively. Eventually, on the applied 45 °C, the OML-SOCE technique has accomplished to a lower RMSE of 0.31 but the RBFNN- BSA, GRNN-BSA, ELM- BSA, and BPNN- BSA methodologies have achieved a higher RMSE of 1.75, 1.81, 2.27, and 0.57 correspondingly.

A brief MAPE results analysis of the OML-SOCE technique for SOC estimation in FUDS cycle is displayed in Fig. 9. The figure outperformed that the OML-SOCE technique has resulted to an effective outcome with the least MAPE. On the applied 0 °C, the OML-SOCE approach has accomplished to a lesser MAPE of 18.53 but the RBFNN- BSA, GRNN- BSA, ELM- BSA, and BPNN- BSA techniques have obtained a higher MAPE of 31.13, 19.56, 34.71, and 20.09 respectively. At the same time, on the applied 25 °C, the OML-SOCE technique has accomplished to a lower MAPE of 11.87 but the RBFNN- BSA, GRNN-BSA, ELM- BSA, and BPNN- BSA techniques have obtained a higher MAPE of 18.54, 16.38, 20.67, and 12.61 respectively. Finally, on the applied 45 °C, the OML-SOCE methodology has accomplished to a minimum MAPE of 9.21 but the RBFNN- BSA, GRNN-BSA, ELM- BSA, and BPNN- BSA approaches have gained a maximum MAPE of 12.84, 12.11, 19.94, and 9.63

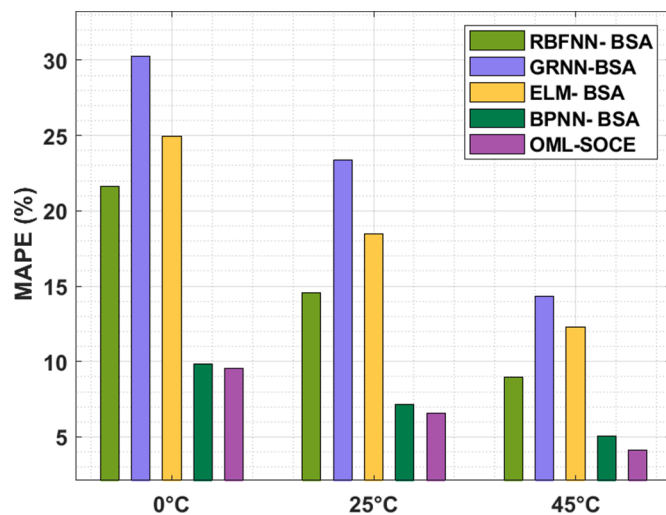


Fig. 7. MAPE analysis of OML-SOCE model under DST cycle.

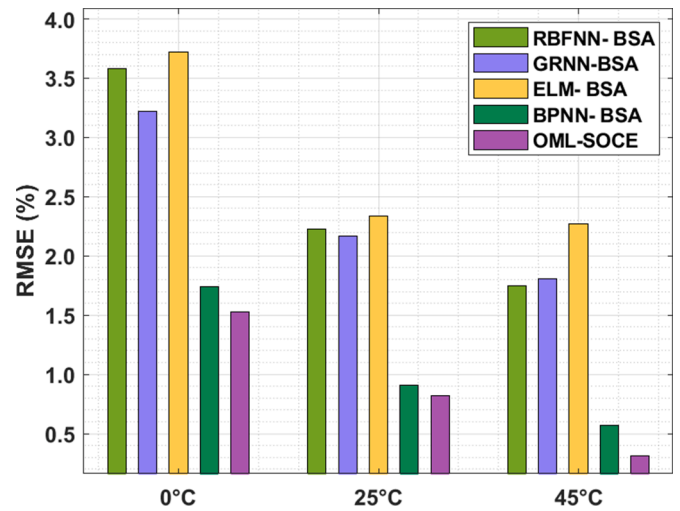


Fig. 8. RMSE analysis of OML-SOCE model under FUDS cycle.

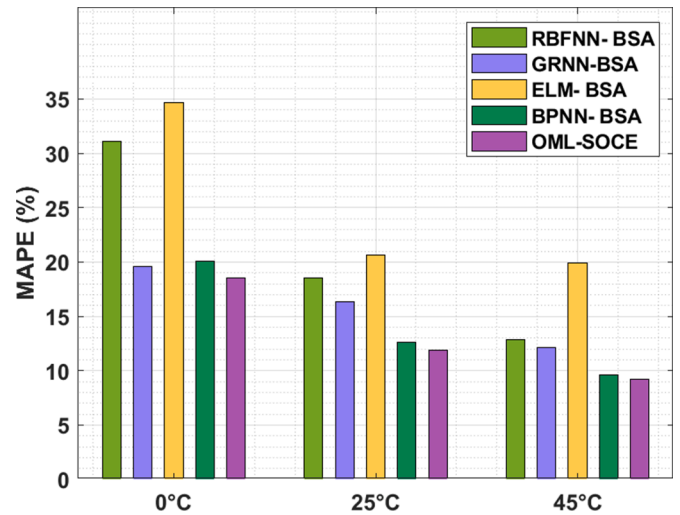


Fig. 9. MAPE analysis of OML-SOCE model under FUDS cycle.

correspondingly.

Table 1 investigates the performance of the OML-SOCE technique with existing techniques in terms of SOC error [24]. The results depicted that the OML-SOCE technique has gained minimal SOC error values under varying temperature levels and cycles. On examining the results under 0 °C, the OML-SOCE technique has accomplished a lower SOC

Table 1
Result analysis of existing with proposed OML-SOCE model for SOC Error (%).

Methods	Temp.	DST Cycle	FUDS Cycle
RBFNN- BSA	0 °C	[-12.1 + 12.3]	[-21.8 + 30.5]
	25 °C	[-7.7 + 8.9]	[-8.6 + 10.2]
	45 °C	[-5.9 + 5.5]	[-5.8 + 9.2]
GRNN-BSA	0 °C	[-13.5 + 8.3]	[-18.7 + 27.8]
	25 °C	[-11.7 + 13.8]	[-8.7 + 11.1]
	45 °C	[-6.1 + 12.6]	[-8.4 + 10.5]
ELM- BSA	0 °C	[-14.5 + 18.5]	[-22.8 + 30.8]
	25 °C	[-10.1 + 9.2]	[-12.7 + 13.9]
	45 °C	[-6.1 + 7.6]	[-10.6 + 16.4]
BPNN- BSA	0 °C	[-8.5 + 8.8]	[-4.8 + 9.8]
	25 °C	[-2.8 + 4.7]	[-3.8 + 4.8]
	45 °C	[-2.1 + 3.2]	[-2.4 + 3.5]
OML-SOCE	0 °C	[-8.0 + 8.4]	[-3.7 + 9.0]
	25 °C	[-2.1 + 3.7]	[-3.2 + 4.0]
	45 °C	[-1.4 + 2.3]	[-1.6 + 3.0]

error of $[-8.0 + 8.4]$ and $[-3.7 + 9.0]$ on the applied DST and FUDS cycles respectively. Followed by, the BPNN-BSA technique has obtained a slightly increased SOC error of $[-8.5 + 8.8]$ and $[-4.8 + 9.8]$. Moreover, the ELM-BSA and GRNN-BSA techniques have gained moderately higher SOC values. Furthermore, the RBFNN-BSA technique has attained poor outcome with the maximum SOC values of $[-12.1 + 12.3]$ and $[-21.8 + 30.5]$ on the applied DST and FUDS cycles respectively. By looking into the above mentioned results analysis, it is apparent that the OML-SOCE technique is found to be effective compared to existing techniques.

5. Conclusion

In this study, a new OML-SOCE approach is derived for the SOC estimation of the Li-ion battery for P2P energy trading in TEM. The OML-SOCE technique includes SSAE based predictive model to determine the proper level of SOC. The SSAE is an enhanced auto-encoder technique that improves any sparsity restrictions from the hidden layer of standard auto-encoder. Besides, the parameter optimization of the SSAE model takes place using the SSA. A comprehensive simulation analysis is carried out and the outcomes are inspected under distinct temperature levels. The experimental results depicted the supremacy of the proposed technique on the recent techniques with respect to different measures. In future, the SOC predictive outcomes can be raised by the use of advanced deep learning and feature selection approaches.

Authors statement

All authors have read and agreed to the published version of the manuscript.

CRedit authorship contribution statement

Subramanian Annamalai: Conceptualization, Writing – original draft. **S.P. Mangaiyarkarasi:** Conceptualization, Data curation, Formal analysis. **M.Santhosh Rani:** Data curation, Formal analysis, Investigation, Methodology. **V. Ashokkumar:** Investigation, Methodology, Project administration, Resources, Supervision. **Deepak Gupta:** Project administration, Resources, Supervision, Validation, Visualization. **Joel JPC. Rodrigues:** Validation, Visualization.

Declaration of Competing Interest

The authors declare that they have no known competing financial interests or personal relationships that could have appeared to influence the work reported in this paper.

Acknowledgements

This work is supported by FCT/MCTES through national funds and when applicable co-funded EU funds under the Project UIDB/50008/2020; and by Brazilian National Council for Research and Development (CNPq) via Grant No. 313036/2020–9.

Data Availability Statement

Data sharing not applicable to this article as no datasets were generated during the current study.

References

- [1] P. Sivaraman, C. Sharmeela, IoT-based battery management system for hybrid electric vehicle, *Artificial Intelligent Techniques for Electric and Hybrid Electric Vehicles* (2020) 1–16.
- [2] A.K. Basu, S. Bhattacharya (Eds.), *Overview of Electric Vehicles (EVs) and EV Sensors*, Springer, Singapore, 2019.
- [3] Q. Zhang, K. Yu, Z. Guo, S. Garg, J.J.P.C. Rodrigues, M.M. Hassan, M. Guizani, Graph neural networks-driven traffic forecasting for connected internet of vehicles, *IEEE Trans. Netw. Sci. Eng.* (2021), <https://doi.org/10.1109/TNSE.2021.3126830>.
- [4] M.H.A. Wahab, N.I.M. Anuar, R. Ambar, A. Baharum, S. Shanta, M.S. Sulaiman, S. S.M. Fauzi, H.F. Hanafi, IoT-based battery monitoring system for electric vehicle, *Int. J. of Eng. Technol.* 7 (2018) 505–510.
- [5] L. Tan, K. Yu, L. Lin, G. Srivastava, J.C. Lin, W. Wei, Speech emotion recognition enhanced traffic efficiency solution for autonomous vehicles in a 5G-enabled space-air-ground integrated intelligent transportation system, *IEEE Trans. Intell. Transp. Syst.* (2021), <https://doi.org/10.1109/TITS.2021.3119921>.
- [6] C. Feng, et al., Attribute-based encryption with parallel outsourced decryption for edge intelligent IoT, *IEEE Trans. Veh. Technol.* 69 (11) (Nov. 2020) 13784–13795, <https://doi.org/10.1109/TVT.2020.3027568>.
- [7] M. Coleman, C.K. Lee, C. Zhu, W.G. Hurley, State-of-charge determination from EMF voltage estimation: using impedance, terminal voltage, and current for lead-acid and lithium-ion batteries, *IEEE Trans. Ind. Electron.* 54 (5) (2007) 2550–2557.
- [8] E. Chemali, P.J. Kollmeyer, M. Preindl, A. Emadi, State-of-charge estimation of Li-ion batteries using deep neural networks: a machine learning approach, *J. Power Sources* 400 (2018) 242–255.
- [9] M. Charkhgard, M. Farrokhi, State-of-charge estimation for lithium-ion batteries using neural networks and ekf, *IEEE Trans. Ind. Electron.* 57 (12) (2010) 4178–4187.
- [10] F. Ding, K. Yu, Z. Gu, X. Li, Y. Shi, Perceptual enhancement for autonomous vehicles: restoring visually degraded images for context prediction via adversarial training, *IEEE Trans. Intell. Transp. Syst.* (2021), <https://doi.org/10.1109/TITS.2021.3120075>.
- [11] X. Hu, D. Cao, B. Egardt, Condition monitoring in advanced battery management systems: moving horizon estimation using a reduced electrochemical model, *IEEE ASME Trans. Mechatron.* 23 (1) (2018) 167–178.
- [12] V. Chandran, K. Patil, C. Karthick, A. Ganeshaperumal, D. Rahim, R. A. Ghosh, State of charge estimation of lithium-ion battery for electric vehicles using machine learning algorithms, *World Electr. Veh. J.* 12 (1) (2021) 38.
- [13] M.A. Hannan, M.H. Lipu, A. Hussain, P.J. Ker, T.I. Mahlia, M. Mansor, A. Ayob, M. H. Saad, Z.Y. Dong, Toward enhanced state of charge estimation of lithium-ion batteries using optimized machine learning techniques, *Sci. Rep.* 10 (1) (2020) 1–15.
- [14] M.S. Sidhu, D. Ronanki, S. Williamson, October. State of charge estimation of lithium-ion batteries using hybrid machine learning technique, in: *IECON 2019-45th Annual Conference of the IEEE Industrial Electronics Society 1*, 2019, pp. 2732–2737. IEEE.
- [15] L. Zhang, M. Zheng, D. Du, Y. Li, M. Fei, Y. Guo, K. Li, State-of-charge estimation of lithium-ion battery pack based on improved rbf neural networks, *Complexity* (2020) 2020.
- [16] Z. Xu, J. Wang, Q. Fan, P.D. Lund, J. Hong, Improving the state of charge estimation of reused lithium-ion batteries by abating hysteresis using machine learning technique, *J. Energy Storage* 32 (2020), 101678.
- [17] J. Tian, R. Xiong, W. Shen, J. Lu, State-of-charge estimation of LiFePO4 batteries in electric vehicles: a deep-learning enabled approach, *Appl. Energy* 291 (2021), 116812.
- [18] M. Anjum, M. Asif, J. Williams, Towards an optimal deep neural network for soc estimation of electric-vehicle lithium-ion battery cells. energy and sustainable futures, in: *Proceedings of 2nd ICESF 2020*, 2021, p. 11.
- [19] T. Zahid, K. Xu, W. Li, C. Li, H. Li, State of charge estimation for electric vehicle power battery using advanced machine learning algorithm under diversified drive cycles, *Energy* 162 (2018) 871–882.
- [20] E. Chemali, P.J. Kollmeyer, M. Preindl, R. Ahmed, A. Emadi, Long short-term memory networks for accurate state-of-charge estimation of Li-ion batteries, *IEEE Trans. Ind. Electron.* 65 (8) (2017) 6730–6739.
- [21] M. Wei, M. Ye, J.B. Li, Q. Wang, X.X. Xu, State of charge estimation for lithium-ion batteries using dynamic neural network based on sine cosine algorithm, in: *Proceedings of the Institution of Mechanical Engineers, Part D: Journal of Automobile Engineering*, 2021, 09544070211018038.
- [22] Z. Han, M.M. Hossain, Y. Wang, J. Li, C. Xu, Combustion stability monitoring through flame imaging and stacked sparse autoencoder based deep neural network, *Appl. Energy* 259 (2020), 114159.
- [23] V. Chaudhary, H.M. Dubey, M. Pandit, J.C. Bansal, Multi-area economic dispatch with stochastic wind power using salp swarm algorithm, *Array* 8 (2020), 100044.
- [24] M.A. Hannan, M.S.H. Lipu, A. Hussain, M.H. Saad, A. Ayob, Neural Network Approach For Estimating State of Charge of Lithium-Ion Battery Using Backtracking Search Algorithm, 6, *Ieee Access*, 2018, pp. 10069–10079.